P 4.7 THERMAL STABILITY OF PARTICLES CONTAINED IN CIRRUS CRYSTALS: AN ANALYSIS OF DATA OBTAINED DURING THE INCA EXPERIMENTS IN NORTHERN AND SOUTHERN HEMISPHERE MIDLATITUDES

J. Ström[(1)], M. Seifert[(1)], R. Krejci[(1)], A. Minikin[(2)], A. Petzold[(2)], Gayet J-F[(3)], F. Auriol[(3)], J. Ovarlez[(4)] and U. Schumann[(2)]

[(1)] Institute of Applied Environmental Research, Stockholm University, Sweden
[(2)] Institut für Physik der Atmosphäre, DLR, Oberpfaffenhofen, Germany
[(3)] Laboratoire de Météorologie Physique, UMR / CNRS n° 6016, Université Blaise Pascal, Clermont-Fd, France
[(4)] Laboratoire de Météorologie Dynamique, Ecole Polythechnique, Palaiseau, France

Data presented below was collected during two field campaigns in spring and fall of 2000 as part of the EU funded project INCA (Interhemispheric differences in cirrus properties from anthropogenic emissions). The first experiment was conducted in March/April from Punta Arenas, Chile (54S) and the second experiment was conducted in October/November from Prestwick, Scotland (53N).

In an related study also presented in this volume (6.3) we showed that presenting the observed properties as a function of crystal number density Ncvi and relative humidity over ice RHi gave a very powerful way of analyzing the in-situ data. In that study we discussed the evolution of cirrus and how a simple model could capture several of the main features observed if assuming gravity waves as the main dynamic forcing. In this study we will make use of the unique feature of the CVI (Counterflow Virtual Impactor) that allows for real-time analysis of the content in cirrus crystals.

The crystals are inertially separated from the ambient air by a probe pointing in the direction of flight. A counter air (air stream directed against the flight direction) prevents ambient gases, aerosols and cloud particles smaller than about 5 μm aerodynamic diameter from entering the probe.

Once the crystal is sampled by the CVI probe the cloud particle is surrounded by a dry, particle free and relatively warm carrier gas (N_2). The condensed water evaporates and the crystal leaves behind a residual particle. These residual particles may be analyzed by different sensors inside the aircraft in real time or by post flight techniques. By counting the residual particles the crystal number density can be inferred. Intercomparisons with concurrent measurements conducted by the FSSP-300, 2D-C and the Polar Nephelometer show that the assumption of a one-to-one relation between the crystal number density and the residual number density is valid.

As part of the INCA experiment, a thermal denuder system was connected to the CVI probe. The schematics in Figure 1 below show this setup. Sample air from the CVI-probe was divided into three different branches and heated to different temperatures before any particles remaining were counted by CPC's.

Corresponding author address: Johan Ström, Inst. of Applied Environmental Research, Stockholm Univeristy, S-106 91 Stockholm, Sweden. E-mail: johan@itm.su.se

The fraction of particles that disappeared after heating the sample air to 125ºC was termed volatile particles. The fraction of particles remaining after heating to 250ºC was termed non-volatile. The remaining fraction was termed semi-volatile particles.

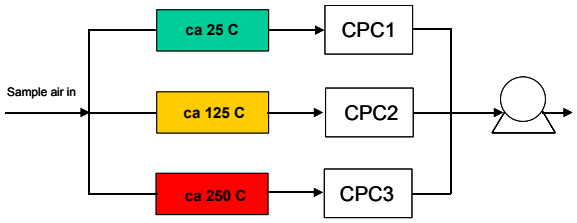

Figure 1. Schematic layout of the thermal denuder system. The sample air comes from the CVI probe.

Figure 2 shows the averaged fraction of volatile particles as a function of relative humidity and crystal number density (Ncvi). The analysis only includes measurements above 6km altitude and at a temperature below 235K. The two panels in Figure 2 clearly show that the two campaigns are systematically different in their average fractions, where the Prestwick campaign (top) display significantly higher fractions of volatile particles compared to the Punta Arenas campaign (bottom).

However, both data sets show a similar trend or gradient in the average properties, where the fraction of volatile particles decrease with increasing humidity and increasing crystal number density. The fraction of semi-volatile particles presented in Figure 3 are very small and the fraction of non-volatile particles presented in Figure 4 are essentially the complement to the volatile particles.

The size distribution measurements of residual particles performed during INCA was done by a combination of CPC, DMPS and OPC in order to cover the size range from 10 nm to about 3 μm diameter. To get a feel for the relative importance of the accumulation mode size range the average fraction of particles larger than 120nm is presented in Figure 5 using the same format as in Figures 2, 3, and 4.

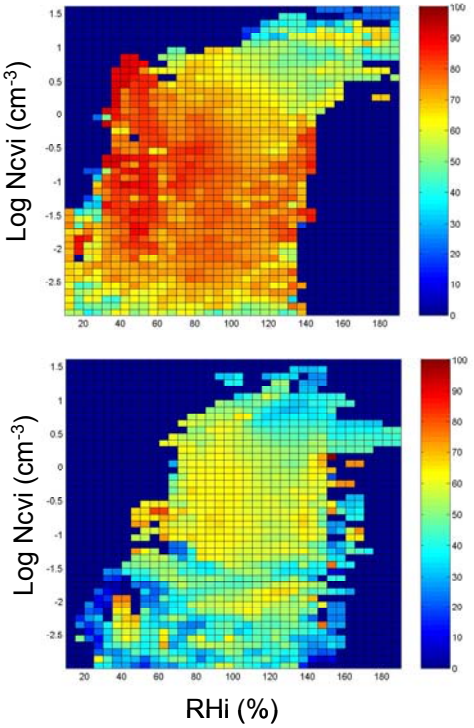

Figure 2. Average volatile particle fraction as function of relative humidity over ice and crystal number density. The Prestwick campaign (top) and Punta Arenas campaign (bottom).

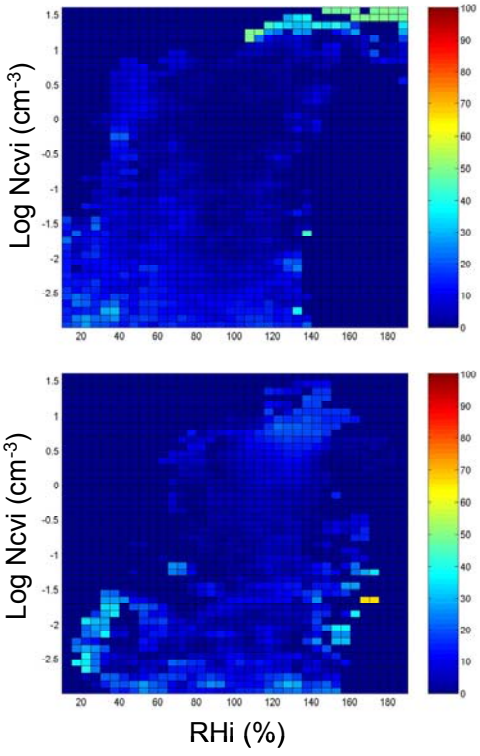

Figure 3. Same as Figure 2 but for semi-volatile particles.

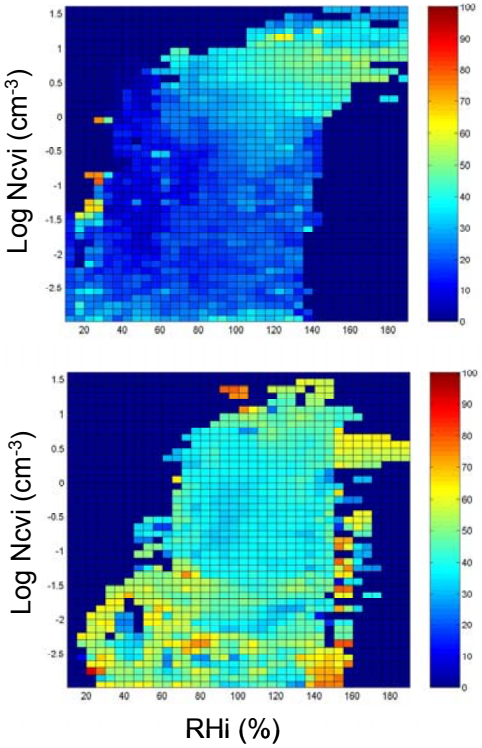

Figure 4. Same as Figure 2, but for non-volatile particles.

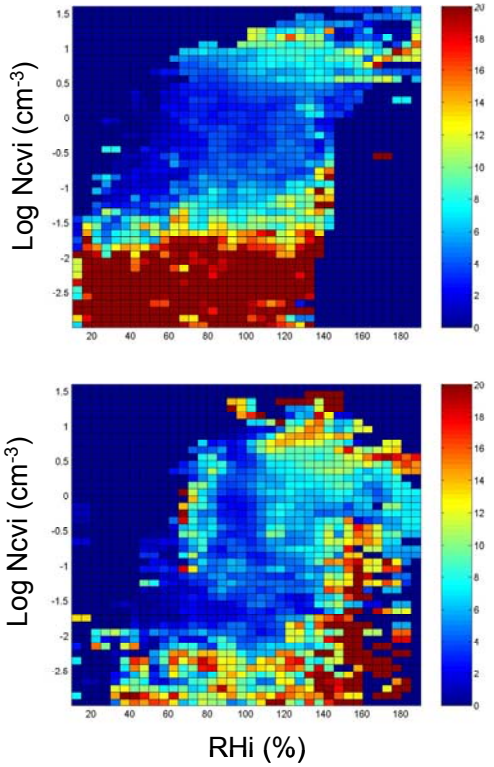

Figure 5. Average fraction of accumulation mode particles in the residual particle size distribution. Prestwick campaign (top) and Punta Arenas (bottom).

Especially at humidities above 100 % the patterns of non-volatile particle fractions and the accumulation mode particles fractions show similar trends with relative humidity and crystal number density, which suggests that the larger residual particles are associated with the non-volatile particles. At low integral residual number densities (less than about 10 per liter), the number of accumulation mode particles becomes more uncertain due to counting statistical problems.

This piece of information of a connection between large residuals and non-volatile particles encourages us to attempt to fit three distributions, each representing a different particle composition, or thermal property, to the observed size distribution. We divide the data into four number density bins (0.1-0.3, 0.3-1, 1-3, and 3-10 cm^{-3}). For each Ncvi bin the average volatile, semi-volatile, and non-volatile fraction was calculated. This will smooth some of the features seen in Figures 2-4, but will still capture the main differences between the two campaigns.

The resulting average fractions are presented in Table 1. These numbers where used to constrain the fitting procedure. To reduce the endless number of possibilities some more constraints were introduced. Volatile and semi-volatile particles were described by one log-normal distribution each, whereas the non-volatile particles were described by three log-normal distributions.

Table 1. Average fraction of particle types as function of crystal number density

Ncvi (cm^{-3})	Volatile (%)	Semi-Volatile	Non-volatile
		Prestwick	
3-10	53	4	43
1-3	64	3	33
0.3-1	73	2	25
0.1-0.3	80	1	19
		Punta Arenas	
3-10	43	16	41
1-3	56	6	38
0.3-1	66	3	31
0.1-0.3	73	2	25

The procedure was such that the non-volatile particles where fitted to the largest particles first and then towards progressively smaller particles until the fraction of particles was expended. The volatile particles were fitted to the smallest particles first and then towards larger particles until the volatile fraction of particles were expended. The semi-volatile fraction was essentially used to fill in gaps not covered by the other two compositions and distributions.

The rationale for this procedure is that volatile particles are assumed to be formed in-situ from gas-to-particle conversion (read sulfuric acid particles), and that the particles therefore enters the distribution from the left side. Semi-volatile particles are the aged aerosol that has had some time to become more or less neutralized (read ammonium sulfate particles) and this mode should therefore be located to the right of the volatile particles.

The non-volatile particles may have a more diverse distribution of sources and is therefore described by three modes representing crustal particles, organic particles, soot etc. Figure 6 shows the result for the Ncvi bin 3-10 cm^{-3}.

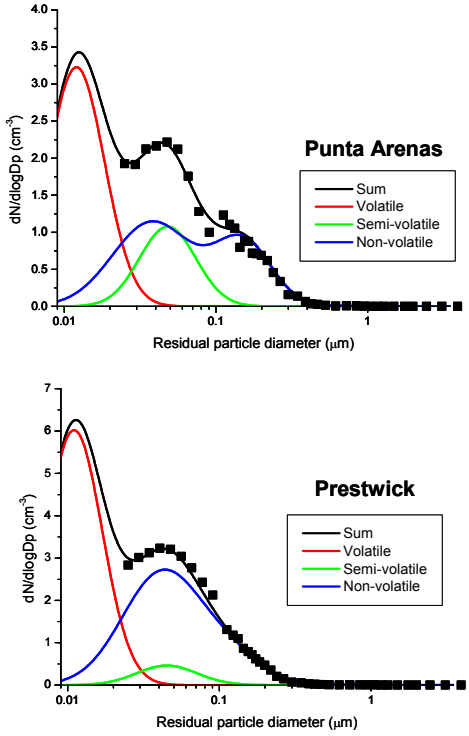

Figure 6. Three particle types fitted to the observed residual size distribution (squares). Crystal number density between 3 and 10 cm^{-3}.

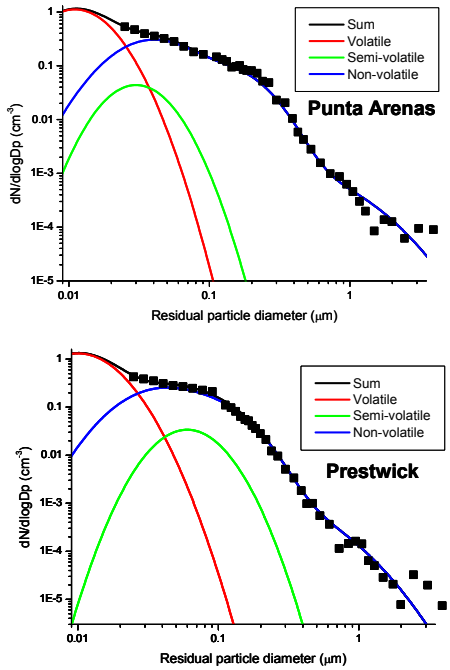

Figure 7. As Figure 6, but on a log-log scale and crystal number densities between 0.1 and 0.3 cm^{-3}.

The distributions at sizes smaller than 25 nm (start of the DMPS size distribution) are constrained by the integral number density for particles larger than 10 nm measured by the CPC. Figure 7 shows the Ncvi bin 0.3-1, but on a log-log plot to highlight the tail towards larger particles, which is unimportant for the number density but is very important for the aerosol volume or aerosol mass

For each of the four Ncvi bins and for each campaign we have calculated the aerosol mass of non-volatile particles from the fitted distributions assuming a particle density of 2 g cm^{-3}. The resulting mass densities are plotted as red symbols in Figure 8. The vertical whiskers represent an uncertainty equivalent of a density between 1.5 and 2.5 g cm^{-3}. The uncertainty is not only in the density but arrives from the uncertainty in the size measurements as well. The horizontal whiskers represent an uncertainty in the number density by 20%.

The derived aerosol mass from the fitted non-volatile distributions is compared to an independent measurement of the mass of absorbing particles. To measure the absorbing particles a custom built instrument that uses the so-called integrating plate method was also connected to the CVI probe. The light from a single source is split in two beams that illuminate a particle filter. Two detectors beneath the filter register the green light transmitted through the filter. Particles are only collected on one side and the differential between the two detectors is a measure of the amount of absorption particles deposited on the filter. A specific absorption coefficient of 10 m^2 g^{-1} was used to convert the absorption signal to a mass concentration.

The data from the absorption measurements are plotted as blue squares in Figure 8. The derived mass of non-volatile particles and the measurements of absorbing particles show similar values and trend as function of crystal number density. This comparison suggests that a significant amount of the non-volatile particles absorb light very efficiently and that the difference between the two campaigns is not so large with respect to this quantity. A finding that is somewhat surprising, considering the much larger anthropogenic sources in the Northern Hemisphere.

The crystal residuals observed in the Southern Hemisphere campaign show a larger fraction of non-volatile particles compared to the Northern Hemisphere. Typically, 30 to 40 % of the residual particles present in crystals in the Punta Arenas campaign remained after heating the sample air to 250ºC. In general the fraction of non-volatile particles increased with increasing relative humidity. The fraction of semi-volatile particles was small in both campaigns.

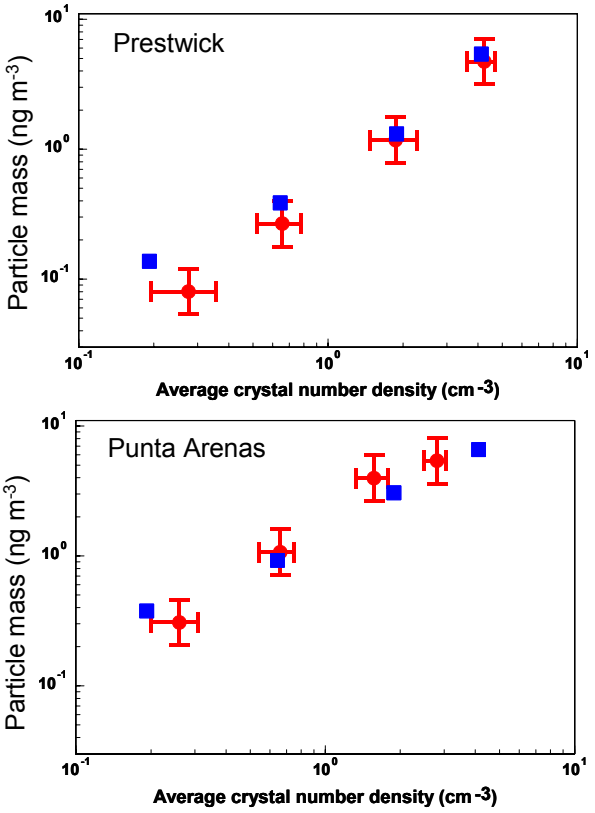

Figure 8. Derived non-volatile residual particle mass as function of the number density (red markings), and the mass of absorbing particles contained in cirrus crystals as function of crystal number density.

The derived non-volatile particle mass as function of crystal number density shows similar values and trends as measurements of absorbing particles contained in the crystals. This suggests that non-volatile particles in cirrus crystals to a large extent are strongly light absorbing particles.

All these data was collected at temperatures below 235K, and the obvious question is how observations presented above may fit with homogeneous nucleation, which is believed to be the main mode of cloud formation at these temperatures. The state of internal/external mixture of the aerosol is not known and it is possible that soluble material on the non-volatile particles still make these particles nucleate through haze droplet formation. The higher the humidity reached in the cloud the larger the fraction of the particles nucleate.